NeuroImage: Clinical 18 (2018) 149–159

Contents lists available at ScienceDirect

NeuroImage: Clinical

journal homepage: www.elsevier.com/locate/ynicl

Dynamic causal modeling revealed dysfunctional effective connectivity in both, the cortico-basal-ganglia and the cerebello-cortical motor network in writers' cramp

Inken Rothkirch[a], Oliver Granert[a], Arne Knutzen[a], Stephan Wolff[b], Felix Gövert[a], Anya Pedersen[c], Kirsten E. Zeuner[a], Karsten Witt[a,d,*]

[a] Department of Neurology, Kiel University, Germany
[b] Department of Radiology, Kiel University, Germany
[c] Department of Psychology, Kiel University, 24118 Kiel, Germany
[d] School of Medicine and Health Sciences - European Medical School, University Hospital of Neurology, Medical Campus University of Oldenburg, 26111 Oldenburg, Germany

ARTICLE INFO

Keywords:
Dynamic causal modeling
Focal hand dystonia
Writer's cramp
Network disorder
Cerebellum

ABSTRACT

Writer's cramp (WC) is a focal task-specific dystonia characterized by sustained or intermittent muscle contractions while writing, particularly with the dominant hand. Since structural lesions rarely cause WC, it has been assumed that the disease might be caused by a functional maladaptation within the sensory-motor system. Therefore, our objective was to examine the differences between patients suffering from WC and a healthy control (HC) group with regard to the effective connectivity that describes causal influences one brain region exerts over another within the motor network. The effective connectivity within a network including contralateral motor cortex (M1), supplementary motor area (SMA), globus pallidus (GP), putamen (PU) and ipsilateral cerebellum (CB) was investigated using dynamic causal modeling (DCM) for fMRI. Eight connectivity models of functional motor systems were compared. Fifteen WC patients and 18 age-matched HC performed a sequential, five-element finger-tapping task with the non-dominant and non-affected left hand within a 3 T MRI-scanner as quickly and accurately as possible. The task was conducted in a fixed block design repeated 15 times and included 30 s of tapping followed by 30 s of rest. DCM identified the same model in WC and HC as superior for reflecting basal ganglia and cerebellar motor circuits of healthy subjects. The M1-PU, as well as M1-CB connectivity, was more strongly influenced by tapping in WC, but the intracortical M1-SMA connection was more facilitating in controls. Inhibiting influences originating from GP to M1 were stronger in controls compared to WC patients whereby facilitating influences the PU exerts over CB and CB exerts over M1 were not as strong. Although the same model structure explains the given data best, DCM confirms previous research demonstrating a malfunction in effective connectivity intracortically (M1-SMA) and in the cortico-basal ganglia circuitry in WC. In addition, DCM analysis demonstrates abnormal reciprocal excitatory connectivity in the cortico-cerebellar circuitry. These results highlight the dysfunctional cerebello-cortical as well as basalganglio-cortical interaction in WC.

1. Introduction

Dystonia is a clinical syndrome characterized by sustained muscle contractions, producing twisting, repetitive, and patterned movements, or abnormal postures. The dystonic syndromes include a large group of diseases that have been classified into various etiological categories, such as primary, dystonia-plus, heredodegenerative, and secondary (Albanese et al., 2013). In addition to the investigation of differences in isolated brain regions between patients and healthy controls, a series of studies indicated abnormalities in brain circuits as the underlying mechanism of focal dystonia with focus on the primary motor cortex (M1), the supplementary motor area (SMA), cerebellum (CB), parts of the basal ganglia - in detail the globus pallidus (GP) and putamen (PU) - as well as the thalamus. On the one hand there is evidence that dysfunctions of a network are embedded in the cortico-striatal pathway (Ibáñez et al., 1999; Islam et al., 2009; Oga et al., 2002; Wu et al., 2010). For instance, abnormal dopaminergic function within the cortico-striatal circuity has been described in dystonia (Simonyan et al., 2017). In

* Corresponding author at: Department of Neurology, Oldenburg University, Evangelisches Krankenhaus Oldenburg, Steinweg 13-17 26122 Oldenburg, 24105 Kiel, Germany
E-mail address: karsten.witt@evangelischeskrankenhaus.de (K. Witt).

https://doi.org/10.1016/j.nicl.2018.01.015
Received 24 August 2017; Received in revised form 9 January 2018; Accepted 15 January 2018
Available online 28 January 2018
2213-1582/ © 2018 The Authors. Published by Elsevier Inc. This is an open access article under the CC BY-NC-ND license (http://creativecommons.org/licenses/BY-NC-ND/4.0/).

addition, dysfunctions in the cerebello-cortical pathway have been detected as well. Neuronal activity in the cerebellum in writer's cramp (WC) is increased (Hu et al., 2006; Preibisch et al., 2001), and therefore the cerebellar influence on the motor cortex possibly leads to a deficit in cortical inhibition and stronger dystonic symptoms (Bradnam et al., 2015). Just recently, Gallea et al. (2018) confirmed the hypothesis of cortico-cerebellar abnormalities in WC. They found an abnormal decrease of GABA-A receptor density in the right cerebellum and the left sensorimotor cortex resulting in the loss of inhibitory cortical control (Gallea et al., 2018). Even in resting-state networks WC patients show a divergent neuronal activation compared to healthy controls. Thus, a reduced positive subcortico-cortical functional connectivity in combination with an increased negative cortico-cerebellar functional connectivity was evident (Dresel et al., 2014). Since primary dystonia is considered a network disorder (Blood et al., 2006; Delmaire et al., 2009; Gallea et al., 2018; Hinkley, 2013; Islam et al., 2009; Oga et al., 2002; Simonyan et al., 2017; Wu et al., 2010; Zeuner et al., 2015) the investigation of the functional connectivity between the nodal points of the network may give new pathophysiological insights. Thus, the aim of the present study was to investigate the movement-dependent pathophysiology of WC while focusing on the effective connectivity within the motor network activated during a finger-tapping task. In contrast to previous studies that focused on isolated brain regions, the purpose of our study was to examine the affected network in a more holistically manner. This approach is crucial to get a closer understanding of the diverging interaction among motor areas in patients with WC compared to healthy subjects. Based on previous literature, we firstly assumed a movement-dependent abnormal activation within the cortico-striatal network comprising the motor cortex, the putamen and the globus pallidus in patients with WC compared to healthy controls (Ibáñez et al., 1999; Oga et al., 2002; Simonyan et al., 2017; Wu et al., 2010). Secondly, we expected diverging cortico-cerebellar network activation (Bradnam et al., 2015; Gallea et al., 2018). We implemented dynamic causal modeling (DCM) to address the question whether the underlying neuronal motor network during finger-tapping is identical in writer's cramp and healthy controls and if so, whether single connections between network regions are different. DCM is a method for network analyses employing effective connectivity and has been introduced by Friston et al. (2003). The advantage of DCM is the possibility to estimate hidden neuronal states based on measuring brain activity, e.g. blood oxygenation level depended (BOLD) signal. Changes within a network analysis depend on the motor performance (Pool et al., 2013). Hence, comparing the functional connectivity of patients suffering from dystonia with matched controls may be confounded by impaired motor performance in dystonic patients. In order to exclude such a confounding factor, we investigated in this study the activity of the motor network, while tapping with the non-affected in WC Patients and controls. We recently demonstrated that WC patients performed a finger-tapping task with the non-affected hand equivalent to controls. Regardless, changes in the motor network were still evident in dystonic patients while performing this motor task with the non-dominant hand (Zeuner et al., 2015).

2. Materials and methods

2.1. Subjects

The results of the structural and functional MRI analysis have been published by Zeuner et al. (2015) previously. In this study, we included fifteen patients suffering from writer's cramp (6 women, mean age of 51.6 ± 11.1 years, range: 35–69) with a mean disease duration of 15.7 ± 8.9 years (range: 3–36 years). Four patients disclosed simple writer's cramp showing symptoms only during writing, while all further patients suffered from complex writer's cramp and even demonstrated dystonic symptoms when performing fine motor tasks other than writing. Further, nine patients exhibited mirror dystonia. The diagnosis of dystonia was established by medical history and by using the Writer's Cramp Rating Scale (Wissel et al., 1996) and the Arm Dystonia Disability Scale (Fahn, 1989). The Arm Dystonia Disability Scale (ADDS) contains seven items that together estimate the impairment of manual skills reported by patients. A score of 100% indicates normal motor function. The final score represents the percentage of normal manual activity. Therefore, a lower ADDS score means the patient suffers from more severe functional impairment. According to the Arm Dystonia Disability Scale, writer's cramp patients exhibited difficulties in other fine motor tasks such as using a computer mouse, using the keyboard of a computer, battening shirts, blouses, using silverware for eating, grasping objects or difficulties with homework or in the job. The mean of the ADDS was equal to 56.4% (± 14.1% SD).

We further used the Writer's Cramp Rating Scale (WCRS) (Wissel et al., 1996) to examine the clinical presentation. Patients were videotaped while writing the German sentence “Die Wellen schlagen hoch” (“The waves are surging high”) ten times without a break between consecutive sentences, and the severity of writer's cramp was analyzed from the video segments (Wissel et al., 1996). A higher total WCRS score (with a maximum score of 30 points) means the patient showed more severe dystonic signs during handwriting. The mean in our sample was equal to 8.8 (± 4.6). Table 1 displays an overview of patients' characteristics. Eighteen age-matched healthy individuals (7 women) with a mean age of 51.1 ± 8.4 years (range: 33–68) served as controls. All participants were right-handed, ascertained through the Edinburgh Inventory (Oldfield, 1971), but in our study they performed

Table 1
Characteristics of included patients suffering from writer's cramp.

Patient ID	Age (y)	Symptom duration (y)	Type of writer's cramp	Last injection (months)	Duration BoNT treatment (y)	Total ADDS score (%)	Total WCRS score	Mirror dysonia
P101	69	9	Complex	4	8	60	10	Yes
P106	49	10	Complex	n.a.	n.a.	68.57	5	Yes
P107	43	9	Complex	60	3	64.29	22	Yes
P108	36	11	Simple	n.a.	n.a.	55.71	8	Yes
P110	60	14	Simple	n.a.	n.a.	51.43	6	No
P112	36	3	Complex	17	0.7	42.85	7	No
P115	56	14	Simple	5	10	60	10	No
P119	35	21	Complex	36	0.5	48.9	14	Yes
P120	58	25	Complex	72	0.25	60	5	Yes
P122	59	13	Complex	120	0.5	51.43	6	No
P123	68	25	Complex	132	0.5	25.71	8	No
P125	55	4	Complex	18	3	81.43	5	Yes
P127	51	19	Complex	3	4	72.86	3	Yes
P128	57	34	Complex	10	2	34.29	12	Yes
P129	42	22	Simple	6	1	68.57	11	No

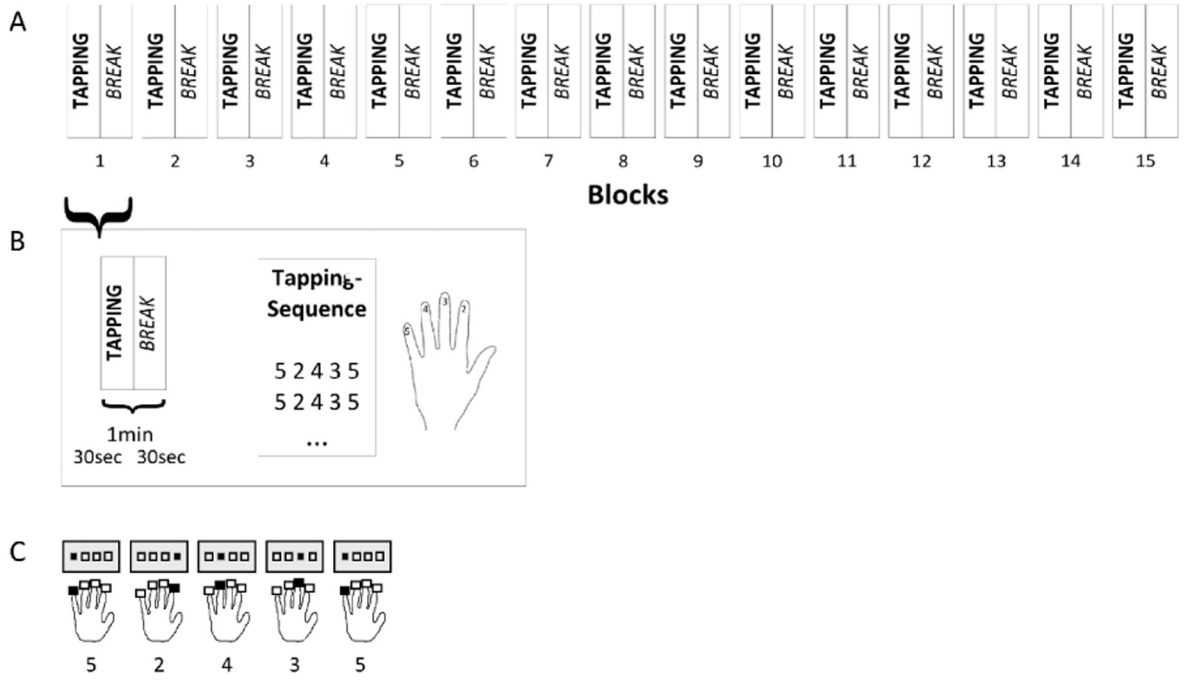

Fig. 1. (A) The experimental design consists of fifteen blocks, whereby (B) each block comprises 30 s of sequence tapping followed by a 30-second pause. (C) Participants tapped the 5-element sequence (5-2-4-3-5) with the left hand, whereby the forefinger corresponds to 2 and the little finger to 5.

a finger-tapping task with the left hand. Participants with any neurological or psychiatric disorder other than writer's cramp, a history of any impairment to the nervous system, as well as musicians and professional typists were excluded from the study. Furthermore, a criterion was that the last botulinum toxin was injected at least 3 months prior to inclusion. All participants had given written informed consent before their participation. The study was approved by the local ethics committee in Kiel and conducted in full accordance with the Declaration of Helsinki.

2.2. Experimental design

Using the fingers of the left hand, which were assigned the numbers 2–5 beginning with the forefinger to tap corresponding numbers on keys, participants repeated a five-element sequence (5-2-4-3-5) on a manual hand device that was part of the Invivo IFIS fMRI system (Invivo, Gainesville, Florida, USA) programmed on E-Prime® software (Psychology Software Tools, Inc., Sharpsburg, USA). The investigator instructed participants to tap as fast and accurately as possible. A block contained 30 s of tapping followed by a rest pause of equal time. This block was repeated 15 times (Fig. 1). During the whole experiment the numeric sequence was displayed to the participants through a mirror within the MRI scanner to minimize the influence of working memory. After each key press, the fixation cross on the screen switched to a circle for 100 ms with no accuracy feedback provided. Prior to the examination in the scanner the task was explained to the participants who then practiced the sequence a few times to make certain they understood the task. For further analysis, timing and accuracy of the key press responses were recorded.

2.3. Image acquisition and processing

Anatomical and functional images were acquired with a 3.0 T whole-body MRI scanner (Achieva 3 T, Philips, Best, Netherlands) provided with an 8-channel head coil in the Neurocenter at Kiel University hospital. An IFIS system was used for stimulus presentation and response recording. For functional MR images a whole-brain echo planar imaging (EPI) sequence with the following parameters was used: repetition time (TR) = 2500 ms, echo time (TE) = 36.4 ms, field of view (FOV) = 216 × 216 × 125.1 mm^3, flip angle = 90°, matrix = 64 × 64, volumes = 360, slices = 38, slice thickness = 3.0 mm, and interslice gap = 0.3 mm. The axial slices were acquired parallel to the anterior-posterior plane. For all subjects, additional three-dimensional (3D) T1-weighted gradient echo MRI scans with sagittal volume excitation were acquired with the following parameters: TR = 7.8 ms, TE = 3.6 ms, FOV = 160 × 240 × 240 mm^3, flip angle = 8°, slices = 160, matrix = 256 × 256, voxel size = 1 × 0.94 × 0.94 mm^3.

The SPM12 (Release 6225) software package (SPM12; Wellcome Department of Imaging Neuroscience, London, http://www.fil.ion.ucl.ac.uk) as well as Matlab Version 8.5 (R2015a) (MathWorks Inc., Natick, Massachusetts, USA) were used for image preprocessing, modeling (DCM) and statistical analysis. The structural T1 images were spatially normalized using the segment function to the standard coordinates of the Montreal Neurological Institute (MNI) space delivered with the SPM12 software. To compensate for movement artifacts during the experiment, the functional EPI images were realigned using the SPM12 two pass realignment procedure (pass 1: register to first image; pass 2: register to mean image). Then, we coregistered the mean image of these realigned EPIs to the corresponding individual T1-weighted image and reoriented all EPIs by the resulting transformation. The T1 aligned EPI images were finally normalized by using the parameters determined in the T1 segmentation step. This step wrote normalized versions of the EPI images (2 × 2 × 2 mm^3) allowing optimized voxel wise analysis of the BOLD time-series and statistical group comparisons. Finally, data were smoothed with a Gaussian kernel filter of 8 mm full-width at half-maximum (FWHM).

2.4. Sequential finger-tapping task

To discover potential differences in behavioral variables between patients and controls, i.e. number of correct tabs and number of correct sequences, we conducted two separate two-factorial analyses of variances (ANOVA) for repeated measurements with the within-subject factor *number of blocks* and the between-subject factor *group* (patients vs. controls). For statistical testing a P-value of 0.05 and less was considered a significant result.

3. Dynamic causal modeling

DCM (Friston et al., 2003) was used to examine the effective connectivity within parts of the motor system activated by finger-tapping. DCM is a method to modulate neuronal activity between brain regions mathematically, whereby each region is described by one time-dependent output ($\dot{z}$) corresponding to the observed BOLD signal in this region. Using a bilinear deterministic model with the neuronal state equation F, changes in neuronal activity over time are modeled as

$$F(\vec{z}, \vec{u}, \theta) = \frac{d\vec{z}}{dt} = \dot{z} = \left(A + \sum_{j=1}^{m} \vec{u}_j B^j\right)\vec{z} + C\vec{u} \quad (1)$$

$$A = \frac{\partial F}{\partial z} = \frac{\partial \dot{z}}{\partial z}\Big| \vec{u} = 0$$

$$B^j = \frac{\partial^2 F}{\partial z \partial u_j} = \frac{\partial}{\partial u_j}\frac{\partial \dot{z}}{\partial z}$$

$$C = \frac{\partial F}{\partial u}\Big|\vec{z} = 0. \quad (2)$$

$\dot{z}$ is the time-dependent state vector containing the neuronal activity in the different brain regions and $\vec{u}$ is the input vector to the system, depending on the experimental design. In a block design a positive value codes the presence of the task and a negative value or zero codes the absence, so that $\vec{u}$ contains two different values. Each dynamic model is defined by three sets of parameters. First, matrix A describes the endogenous coupling between regions regardless of the actual experimental condition and is therefore condition-invariant. Off note, the endogenous coupling parameters do not refer to resting state activity within the network as the BOLD signal measured during tapping overlaps the rest periods of 15 s. In such a short time, the motor system does not reach a resting state. Friston et al. (2003) refers to matrix A as effective connectivity, that is, the influence one neuronal system (brain region) exerts over another in terms of inducing a response $\frac{\partial \dot{z}}{\partial z}$ in the mean of a change in neuronal activity. In regard to the design we used here, the parameters of matrix A reflect the strength of the connections between the regions of the motor system without the influence of tapping. Second, the B^j-matrices contain the parameters for changes in coupling between the motor regions induced by the j-th input of the motor task. Therefore, these matrices can be interpreted as the modulation of the effective connectivity by an external influencing factor, which is the finger-tapping task in this study. Parameters of these B^j-matrices indicate how strong finger-tapping influences the coupling between different regions of the motor system. Thus, to differentiate between matrix A and B the most relevant aspect to keep in mind is, that A represents the general connection strengths between regions. Matrix B adds the influence of tapping on these connections, which changes the strength of the coupling between the regions. Finally, matrix C represents the influences of direct extrinsic inputs ($\vec{u}$) to the system. All parameters (A, B^j, C) of the bilinear deterministic model are integrated in θ. For a more expedient interpretation of the results it is appropriate to forego the splitting of the model parameters in matrix A and B. Instead, one can aggregate the respective values. We consider this as a permissible method as the neuronal state equation F is a linear combination of the model parameters. Therefore, we calculated the addition for matrix A and B.

3.1. Regions of interest (ROIs)

The aim of our study was to investigate the movement-dependent, but symptom-independent interactions in terms of effective connectivity among the right motor cortex (M1), the right supplementary motor area (SMA), the right putamen (PU), the right globus pallidus (GP) and the left cerebellum (CB) while subjects performed the task with their left and therefore unaffected hand. As it is the first DCM analysis in patients with WC, we intended to define a simple model. Therefore, we restricted the analysis to the contralateral motor areas and the ipsilateral cerebellum as effective connectivity using this paradigm with relation to the clinical manifestation of focal dystonia. The regions were chosen under consideration of various general theoretical motor learning models (Doyon et al., 2009; Hikosaka et al., 2002) and took the findings of affected regions within the motor network in writer's cramp into account. To extract time series from significant voxels in each region of interest (ROI) in the tapping > rest contrast, subject-specific sphere centers were defined as the closest suprathreshold voxel ($P < .001$) to the coordinates of the second level analysis over all subjects (mean effects of tapping). For participants with neuronal activation under the mentioned threshold in up to two regions of interest, we reduced the threshold to $P < .01$. The individual time series were then computed as the first eigenvariate across all suprathreshold voxels within 6 mm (M1, SMA, CB) or, as applicable, 4 mm (PU, GP) radius from the sphere center and adjusted for effects of no interest, namely, the movement parameters. DCM as a method to analyze effective connectivity assumes that all data were acquired at the same time. Friston et al. (2003) exhibited that DCM is robust to slice-timing differences in block designs of up to 1 s. However, TR here was longer. Therefore, we inverted the normalized coordinates of the ROIs to identify the exact slice where each region was located and thereby received the exact slice timing (Kiebel et al., 2007).

3.2. DCM specification and Bayesian Model Selection

Hypotheses about the task-invariant and therefore endogenous connectivity are required for specifying the structure of different dynamic causal models. Further, one needs an assumption about the effective connectivity driven by the task and the input nodes that are affected by tapping. We conducted an analysis in two steps: First, we searched for the best endogenous connectivity network with the appropriate input node (specifying matrices A & C; B = 0) followed by the determination of affected connections by tapping (specifying the B matrix).

3.2.1. First step: specifying a network of endogenous connectivity with input nodes

For the specification of different model structures we chose the motor network's interconnection of healthy subjects as a basis (model 1). Based on the current understanding of the basal ganglia and the cerebellar motor circuits in writer's cramp, we assumed that three different possible model structures reflect the abnormalities of the endogenous connections between regions of the motor network as depicted in Fig. 2. It is important to keep in mind, that connections between regions in dynamic causal models do not necessarily reflect neurobiological connections. In this case, the connection between the cerebellum and motor cortex is not a direct one in the sense of neurobiology as this pathway passes the thalamus.

→ **Model 1** is derived from the basal ganglia and cerebellar motor circuits of healthy subjects (Alexander and Crutcher, 1990), where the cortical motor areas communicate with the cerebellum as well as with the basal ganglia by affecting the putamen that triggers the globus pallidus and sends the signal back to cortical motor areas via the thalamus. This model reflects the cortico-basal ganglia and cortico-cerebellar circuits as well as their interaction in healthy subjects.

→ **Model 2** reflects the assumption of a cortico-basal ganglia circuit dysfunction in writer's cramp and other types of focal dystonia (Blood et al., 2006; DeLong, 1990; Granert et al., 2011). Therefore, we reduced model 1 by the connections from M1 to the putamen and to the pallidum - M1 path.

→ **Model 3** refers to the postulated cortical-cerebellar circuit maladaptation that may be inherent in focal hand dystonia (Bradnam et al., 2015; Delmaire et al., 2007; Filip et al., 2013; Hubsch et al.,

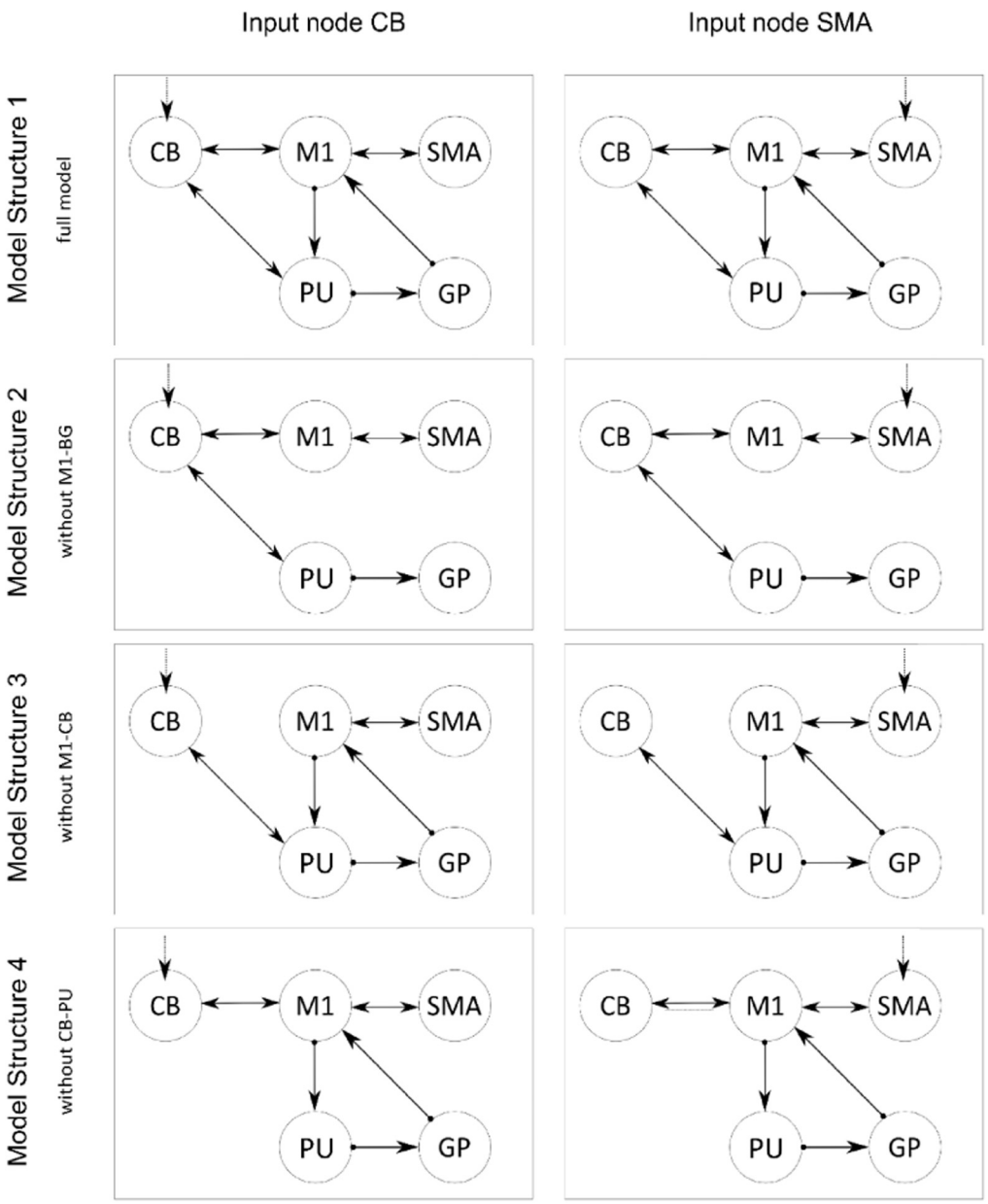

Fig. 2. Schematic illustration of the cerebellar and basal ganglia motor loops comprising the five regions of interest: primary motor cortex (M1) and supplementary motor area (SMA) on the cortical level, putamen (PU) and globus pallidus (GP) on the subcortical level, as well as the cerebellum (CB).

2013; Odergren et al., 1998) and reflects a reduction in the appropriate connections from model 1 again.

→ **Model 4** takes further assumption about network dysfunction in writer's cramp into account concerning the basal ganglia-cerebellar connection (Filip et al., 2017; Neychev et al., 2008).

As the cerebellum (Tzvi et al., 2014; Tzvi et al., 2015) and the SMA (Pool et al., 2013; Rehme et al., 2013; Wang et al., 2011) have been discussed as potential input nodes (matrix C) of the task to the motoric system, we included both areas in our analysis. So each of the four models reflects different aspects of network theory in writer's cramp and has been combined with either the supplementary motor area or the cerebellum as an input node.

After estimating each model for all subjects we conducted in this first step an analysis to draw inference on the model structure regarding the endogenous connections and the input node on group level via Bayesian Model Selection (BMS), which is an established statistical procedure based on the computation of an approximation to the model evidence $p(y|m)$. This probability gives information about how likely data y is under the assumption of a certain model m. For our data we chose a random effects analysis (RFX) BMS implemented in SPM12, which does not, in contrast to a fixed effects analysis (FFX), assume an identical optimal model structure in the population and is therefore more robust against outliers (Stephan et al., 2010). When performing RFX BMS the recommendation is to use family-level inference, because RFX BMS results may possibly be incorrect (Penny et al., 2010). The eight specified models can be separated into two families: First, the structure family, determining the different connectivity patterns and containing four types of models, and second, the input family, referring to the different input nodes and containing two types of models. We preferred an interface model of both family analyses, that is, the model with the highest posterior probability of generating the data was the "winner model" of step one.

3.2.2. *Second step: defining possible paths of effective connectivity*

In the second step of the analysis we defined the matrix determining possible connections affected by tapping, namely, the effective connectivity matrix (B) of the motor system while tapping. Therefore, we took over the "winner model" from the first step and applied it to the groups. We then equated the appropriate matrix of endogenous

connectivity to the matrix of effective connectivity, as each connection required for the task-invariant motor network of the tapping task can potentially be modeled by tapping. This model with completed and defined model matrices was inverted and estimated again for each subject.

3.3. Parameter averaging

Before averaging the subject specific DCMs, the stability of the individually estimated DCMs was checked by computing the Lyapunov exponent of each endogenous connectivity matrix (A), which provides a mathematical degree of stability of a differential equation system's solution (Goldhirsch et al., 1987). Since dynamic causal models are computed on the single subject level, the model parameters for each participant are individually different. As we consider the posterior parameters to be estimates of an underlying true parameter that is the same for all healthy subjects or patients, we conducted a fixed-effects averaging. So these individual connectivity parameters were entered into a fixed-effects (FFX) group level analysis resulting in one averaged DCM per group using a Bayesian approach again, so-called Bayesian Parameter Averaging (Kasess et al., 2010). Further, we computed t-tests on group level adjusted for alpha inflation within each matrix to test whether the averaged parameters differed significantly from zero and then compared the corresponding parameters between the groups to identify potential group differences.

4. Results

4.1. Behavioral results of the sequential finger-tapping task

The ANOVA for the *number of correct tabs* as a repeated measurement including the within-subject factor *number of blocks* and the between-subject factor *group* revealed a main effect of *number of blocks* ($F_{14,434} = 35.38$; $P < .001$; Fig. 3A) but no significant differences in behavior between patients and controls ($F_{1,\ 30} = 0.571$; $P < .456$; Fig. 3A). The second ANOVA with the *number of correct sequences* as a repeated measurement pointed to a very similar outcome structure with a main effect of *number of blocks* ($F_{14,434} = 20{,}16$; $P < .001$; Fig. 3B) and again no *group* differences ($F_{1,\ 30} = 0.367$; $P < .549$; Fig. 3B). Fig. 3 shows an overview of the behavioral data. In addition to statistical analyses of behavioral data, the investigator monitored the finger-tapping through a mirror and interviewed the patients after the experiment whether they had dystonic symptoms during tapping or at rest. None of the patients reported dystonic symptoms during the experimental procedure.

Table 2
Extract from main effects of tapping in all subjects. Whole brain cluster peaks after correction for multiple comparisons ($P < .05$; FWE corrected).

Region	Left hemisphere				Right hemisphere			
	x	y	z	t-Value	x	y	Z	t-Value
Precentral	−50	2	40	11.93	56	8	36	11.64
Postcentral	−62	−18	24	12.77	56	−18	38	13.18
Inferior parietal	−44	−30	40	14.31	42	−42	46	13.67
Superior temporal	−52	−36	18	10.53	60	−30	20	10.45
Middle frontal	−38	38	22	6.17	34	50	2	5.61
Supp Motor Area	−8	4	62	13.63	8	12	60	9.69
Cerebellum 6	−20	−56	−24	17.19	20	−56	−24	13.70
Putamen					26	2	8	10.98
Pallidum	−22	0	0	9.22				

4.2. Neural activity during finger-tapping

Finger-tapping was associated with increased BOLD signals in all regions of interest as well as in further tapping-associated areas ($P < .05$, FWE corrected). For an overview see Table 2. In Fig. 4 five ROIs and the distribution of the subject-specific sphere centers are displayed. We chose those ROIs that were defined as the closest suprathreshold voxel ($P < .001$, uncorrected) to the predefined ROI center. For participants with neuronal activation below the mentioned threshold in up to two regions of interest, we reduced the threshold to $P < .01$. This procedure was necessary for six subjects with small BOLD signal in two regions and three subjects in one region. Further, we limited the sphere centers for all subjects and ROIs to a Euclidean distance under 10 mm.

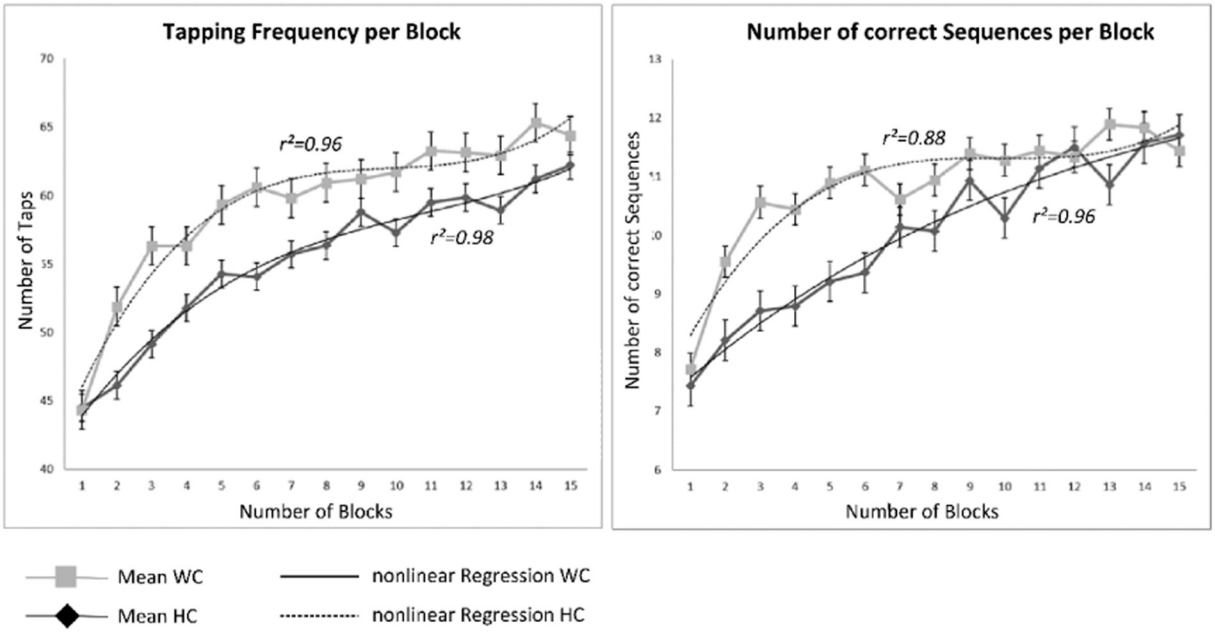

Fig. 3. Behavioral data for controls and patients. The left panel shows the mean number of correct taps per block (± SEM), the right panel the mean number of correct sequences per block (± SEM), whereas the light grey line represents the controls (squares) and the dark line the patients (circles). Additionally, the nonlinear regression curves (polynomial regression of 3rd order) are displayed. A significant increase in the number of correct taps over blocks can be found in patients ($r^2 = 0.98$) and controls ($r^2 = 0.96$) as well as a significant increase in the number of correct sequences (patients: $r^2 = 0.96$; controls: $r^2 = 0.88$).

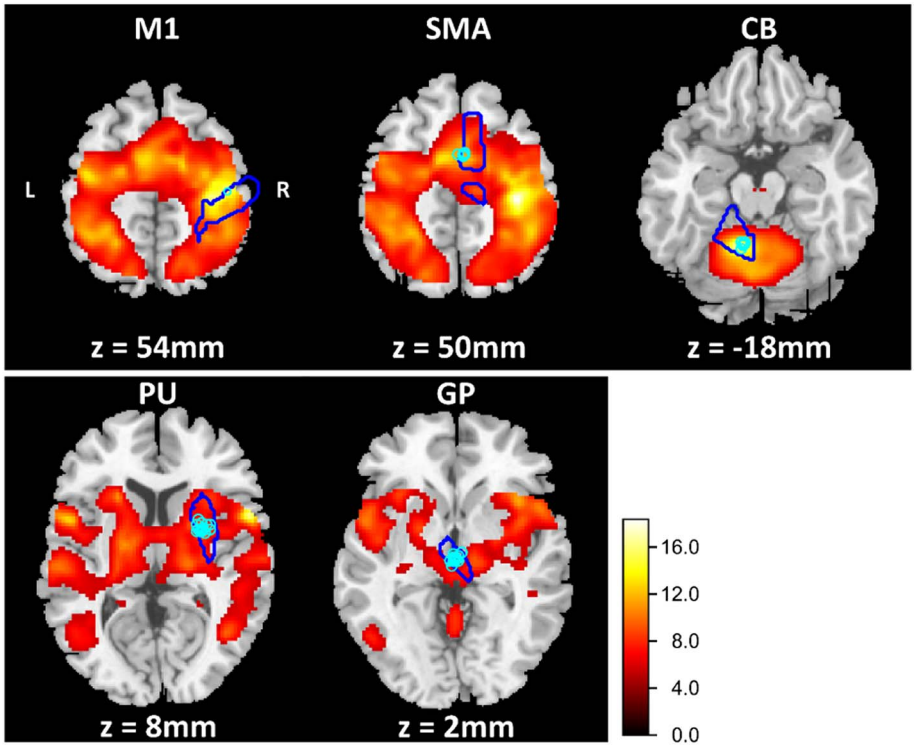

Fig. 4. Statistical maps of the functional magnetic resonance imaging (fMRI) analysis from the finger-tapping task including all subjects for the tapping > rest contrast (P < .05, FWE corrected). The legend depicts t-values. The cyan contours depict the ROIs specified through the AAL Atlas. The blue points show the distribution of the subject-specific sphere centers. All individual centers lay within a sphere of 10 mm Euclidean distance.

Table 3
Cluster peaks of significant regions for the contrast HC > WC while tapping (P < .001; uncorrected).

Region	Left hemisphere					Right hemisphere				
	x	y	z	t-Value	Cluster size	x	y	z	t-Value	Cluster size
Supp Motor Area						10	2	62	4.00	22
Putamen	−24	2	2	3.32	444	32	−6	6	3.50	22
Pallidum	−14	4	4	4.46	444	22	0	6	4.12	94

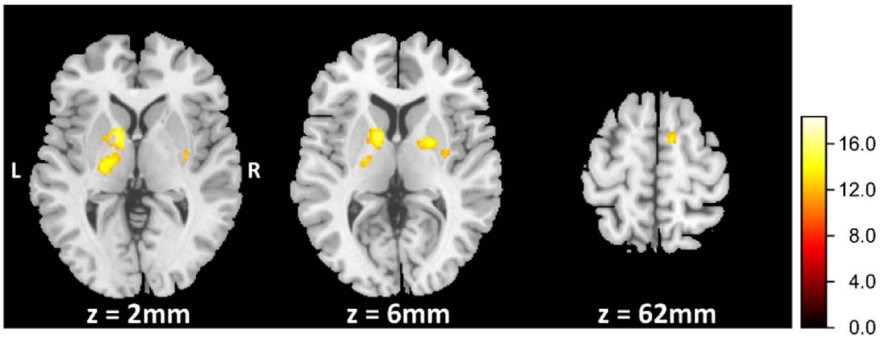

Fig. 5. Statistical maps of the functional magnetic resonance imaging (fMRI) analysis of the finger-tapping task. The legend depicts t-values. Patients exhibited reduced blood oxygen level-dependent (BOLD) signal in the bihemispheric putamen and globus pallidus (z = 2 mm and z = 6 mm) as well as in the right supplementary motor area (z = 62 mm). Figure shows the results of the whole-brain analysis without any masking (P < .001; uncorrected).

Additionally, we found significant differences between healthy controls and focal hand dystonia in the right supplementary motor area, bilateral globus pallidus, as well as bilateral putamen (Table 3). In these areas writer's cramp showed significantly decreased BOLD signals compared to healthy controls. Fig. 5 displays three different transverse cross sections corresponding to the regions where the BOLD response differ between patients and controls.

4.3. DCM analysis

4.3.1. Bayesian Model Selection

As we described in the methods section, we conducted the network analyses in two steps, first identifying the best model structure of endogenous connectivity out of eight previously specified models. Using random effects Bayesian Model Selection (RFX BMS), the model reflecting the basal ganglia and cerebellar motor circuits of healthy subjects with the cerebellum as the input node (Model 1, Fig. 2) showed the highest expected posterior probability (exp_r) of the eight tested models in both groups as it was the intercept model of both “winner” families (HC: $exp\_r_{CB} = 0.93$ $exp\_r_{full} = 0.72$; WC: $exp\_r_{CB} = 0.94$, $exp\_r_{full} = 0.74$). This led us to conclude that this model is most likely the generative model of the given data. Further results of the RFX BMS procedure can be seen in Fig. 6. The analysis of effective connectivity's stability via the Lyapunov exponent resulted in no exclusion. Thus, 18 individual parameter sets of the “winner” DCM were averaged, allowing us to receive a second level DCM in the control group. The same

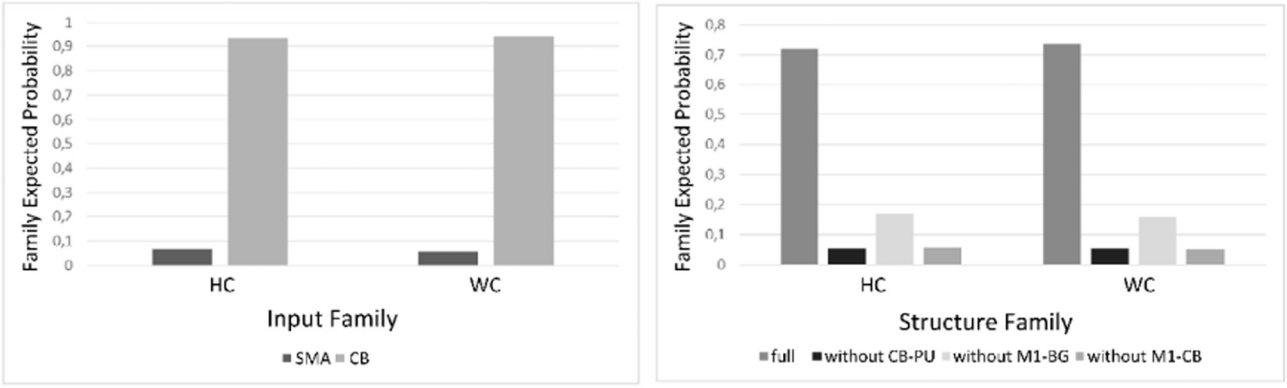

Fig. 6. (A) Family expected posterior probability for the input family, indicating a strong emphasis for the cerebellum as the input node in both groups (HC: $exp\_r_{CB} = 0.93$; WC: $exp\_r_{CB} = 0.94$). (B) The result of the family-wise BMS procedure concerning the model structure resulted in favor of the fully connected model again in both groups (HC: $exp\_r_{full} = 0.72$; WC: $exp\_r_{full} = 0.74$).

procedure was exerted with 15 parameter sets in patients.

4.3.2. Connectivity analysis of the motor network

4.3.2.1. Endogenous coupling. Table 4 displays the group-wise averaged connectivity parameters for the endogenous connectivity (matrix A) between the motor regions in the "winner" model. These parameters reflect changes between brain regions independent of experimental input. The parameter values characterize the connections' strength and their rate of change between the respective regions. Positive parameters are interpreted as facilitation, whereas negative parameters suggest an inhibition of neural activity. Most connectivity parameters in both groups showed significance strength ($P < .05$, Bonferroni corrected). This points to relevant connectivity between regions in the motor system in patients as well as in controls. Merely, the connections from the motor cortex to the putamen and to the cerebellum in the patient group showed connectivity strengths close to zero and therefore failed to reach significance. This finding indicates a loss of intrinsic connectivity between the relevant regions in patients comparing with healthy controls ($t > 3.31$ in HC).

Several differences in the endogenous connectivity ($P < .05$, groupwise Bonferroni corrected for matrix A) occurred between writer's cramp and healthy controls: The HC group showed significant facilitating connections from M1 to putamen and to CB while the same connections failed to be significant in the patient group (Table 4, Fig. 7). However, WC patients had stronger facilitating endogenous connectivity in the CB-M1, CB-Put and Put-CB connections in comparison to HC (Table 4, Fig. 7).

Table 4
Task invariant (A-matrix) coupling parameters in 1/s of the averaged DCMs ($P < .05$, Bonferroni corrected) within each group and differences in endogenous connectivity parameters between patients and controls ($P < .05$, Bonferroni corrected separated by matrices). The difference contrast was defined as $parameter_{HC}$–$parameter_{WC}$. A significant t-value greater than zero indicates a less strong influence of the connection in the patients' model. A significant t-value smaller than zero indicates a stronger influence of the connection in the patients' model.

Connection	WC (n = 15)		HC (n = 18)		Group differences
	Parameter	t-Value	Parameter	t-Value	t-Value
M1-SMA	2.21*	8.47	1.85*	7.73	−15.67*
M1-PU	*0.05*	0.03	0.79*	3.13	15.71*
M1-CB	*0.19*	0.45	1.38*	5.56	16.78*
SMA-M1	0.72*	2.71	0.67*	2.78	−2.52*
PU-GP	2.21*	8.42	2.10*	8.75	−2.83*
PU-CB	1.00*	3.70	0.76*	2.97	−4.62*
GP-M1	−1.34*	−5.34	−1.27*	−5.57	1.71*
CB-M1	0.99*	3.78	0.80*	3.34	−19.87*
CB-PU	1.72*	6.59	1.59*	6.62	−5.78*

* $P < .05$ (Bonferroni corrected seperated by matrices).

4.3.2.2. Task-dependent coupling. The strength of effective connectivity exerted over the motor system while tapping is significant in all tested connections for both groups. However, it differs between groups in a few points (Table 5, Fig. 7). The connectivity between M1 and putamen as well as M1 and cerebellum is more strongly influenced by tapping in WC than in HC. However, the intracortical connection from M1 to SMA is less facilitating in patients. In addition, the inhibiting influence originating from the globus pallidus to M1 is less strong in patients than in controls as well as the facilitating influence the putamen exerts over CB and CB exerts over M1. Further, our analysis identified the cerebellum as input node to the motor system for both groups with no significant difference between the connection strength.

4.3.2.3. Integration of endogenous coupling and the influence of tapping on the motor system. We outlined in the methods section that it is possible to sum up matrix A (Table 4) and B parameters (Table 5) as the bilinear deterministic model integrates them into a linear combination. This procedure results in one parameter for every connection within the model and point the interpretation to more abstract and therefore clinical relevant aspects of the pathophysiological differences between patients and controls. In this study, this approach led to a lower facilitating bidirectional influence between M1 and SMA in WC. For the cortico-basal ganglia circuit, the inhibition M1 exerts over PU and PU exerts over GP was higher in WC, but GP inhibited M1 less strong. In the cortical-cerebellar loop we found increased bidirectional facilitation in WC compared to HC, while the interaction between CB and PU was less facilitating.

5. Discussion

The present study explored the effective connectivity of the motor network in patients with writer's cramp and healthy controls during continuous finger-tapping with the non-dominant and therefore non-affected left hand. Analysis of behavioral data revealed no group differences. Patients and healthy controls showed no significant differences in the number of correctly tapped sequences and frequency. Conversely, we detected differences in functional imaging analysis and in the effective connectivity. Dynamic causal modeling (Friston et al., 2003) was used in a network including the right motor cortex, putamen, globus pallidus and SMA as well as the left cerebellum. DCM treats the brain as a nonlinear and - in our case - deterministic system, whose neural activity changes through an external input, e.g. finger-tapping. This in turn leads to a change in the measured BOLD signal (Friston et al., 2003). Random Effects Bayesian Model Selection across a predefined set of models was used to assess the optimal individual model

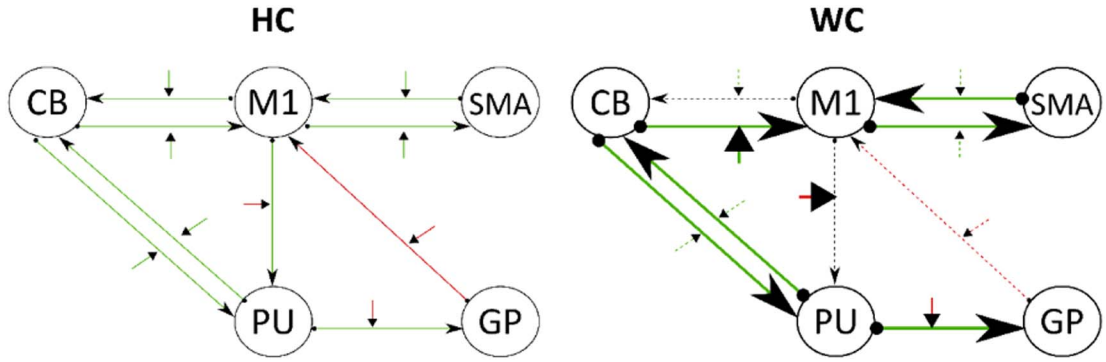

Fig. 7. The left panel depicts the effective connectivity of the motor system in healthy controls. The arrows between two regions refer to the tapping invariant connectivity, while the small arrows perpendicular to those mirror the tapping dependent connectivity. Green arrows (positive parameters) refer to facilitation of neural activity, while red ones (negative parameters) reflect inhibition. The right panel shows the effective connectivity of writer's cramp as well as the differences to the healthy controls' model. Thick arrows depict significant more facilitation or inhibition for the WC model while dotted lines refer to significant less influence in comparison to HC. Black dotted lines are non-significant connections. All tests were significant on $P < .05$ (Bonferroni corrected separated by matrices).

Table 5
Tapping-dependent (B-matrix) coupling parameters in 1/s of the averaged DCMs ($P < .05$, Bonferroni corrected) within each group and differences in these parameters between patients and controls ($P < .05$, Bonferroni corrected separated by matrices). The difference contrast was defined as $parameter_{HC}$–$parameter_{WC}$. A significant t-value indicates an influence of the connection in the patients' model.

Connection	WC (n = 15)		HC (n = 18)		Group differences
	Parameter	t-Value	Parameter	t-Value	t-Value
M1-SMA	3.57*	13.39	6.91*	28.53	21.47*
M1-PU	−5.06*	−20.11	−4.17*	18.26	6.68*
M1-CB	9.50*	36.08	6.62*	27.24	−14.77*
SMA-M1	0.53*	1.71	0.86*	3.34	3.92*
PU-GP	−7.31*	−29.36	−6.86*	−30.29	*1.66*
PU-CB	2.10*	7.15	4.45*	17.78	9.21*
GP-M1	−1.70*	−7.12	−3.96*	−17.44	−15.37*
CB-M1	1.91*	7.34	2.03*	8.56	10.84*
CB-PU	1.56*	5.85	1.74*	7.15	3.25*

* $P < .05$ (Bonferroni corrected seperated by matrices).

structure in both groups followed by inference on the parameter level. Our analysis revealed two main findings: (1) we found diverging effective connectivity in the cortico-cerebellar loop and in the cortico-basal ganglia pathway between HC and WC. (2) The interactions between the cerebellum and the basal ganglia showed a pathophysiological divergence as well.

5.1. Deviations in the cortico-basal ganglia and the cortico-cerebellar loops

The advantage of this study in comparison to previous imaging studies is that we were able to investigate a comprehensive motor dependent network activity during finger-tapping. Furthermore, the effective connectivity in our study was investigated bidirectional that gives us a differential insight into the pathophysiology of dystonia in contrast to other techniques such as fMRI, VBM or DTI analyses. Several different imaging studies with controversial results demonstrated the involvement of the cerebellum in writer's cramp (Delmaire et al., 2007; Peller et al., 2006; Preibisch et al., 2001; Wu et al., 2010). However, the connectivity between the cortex, the cerebellum and the basal ganglia has not been described in any of those studies. Connectivity in patients with WC has been examined in the absence of task, which is resting state fMRI. While two studies describe a deviation in subcortical-cortical functional connectivity in writer's cramp (Dresel et al., 2014; Mohammadi et al., 2012), functional connectivity has been reduced in the cerebellar and the basal ganglia network in a more recent analysis (Mantel et al., 2018). Abnormal anatomical connectivity of the cortico-subcortical sensorimotor structures in WC patients has also been described previously, but did not include the cerebellum (Delmaire et al., 2009). Therefore, the new aspect in our study is the demonstration of activity dependent bidirectional connectivity abnormalities during a motor task that included not only one of the structures such as basal ganglia, the cerebellum or the motor cortex, but all structures involved in the pathophysiology of WC. Here, we detected abnormal effective connectivity within bidirectional connections from the motor cortex to the cerebellum and the basal ganglia in WC patients, a finding that fits well with the results from those previous studies. One of the most striking divergences in our network analyses between writer's cramp and healthy controls was the strongly reduced inhibition the globus pallidus exerts over the motor cortex. This is in accordance with the finding of a decrease in GABA in sensorimotor cortex and the lentiform nuclei (Levy and Hallett, 2002). It is conceivable that the impaired center surround inhibition in the basal ganglia (Beck et al., 2008) accounts for this decreased inhibitory influence of the globus pallidus to the motor cortex and therefore causes the loss of inhibition in M1 (Beck et al., 2008; Hallett, 2011; Levy and Hallett, 2002; Ridding et al., 1995). As a result, dystonic co-contraction may occur in writer's cramp. In concordance with previous studies showing a hyperactivity of the basal ganglia (Peller et al., 2006) the putamen effects the globus pallidus stronger in writer's cramp. Besides these pathophysiological divergences in the interaction between the basal ganglia and the motor cortex our analyses resulted in the pathophysiological involvement of the cortico-cerebellar circuity. Divergent resting state functional connectivity within the cortico-cerebellar loop was found in focal hand dystonia (Hinkley, 2013) and other types of focal dystonia (Haslinger et al., 2017). During tapping we found a slightly stronger facilitation the cerebellum exerts over the motor cortex. However, M1 facilitates the cerebellum significantly stronger in writer's cramp. Future studies need to answer the question, whether the reduction of self-inhibition in M1 might cause the divergence in the facilitating influence the motor cortex exerts over the cerebellum. Recently, Gallea and colleagues found an impaired GABAergic neurotransmission in the cerebellum and the sensorimotor cortex that could explain the loss of inhibitory control in focal hand dystonia (Gallea et al., 2018). It is also conceivable that increased facilitation in the cerebellum reflects a compensatory phenomenon in a deficient cortico-striato-pallido-thalamo-cortical circuit in focal hand dystonia. This has been assumed in hereditary forms of dystonia (Carbon et al., 2008). The cerebellum has been considered to play a role in tuning movement preparation, while the basal ganglia are supposed to inhibit involuntary movements and adapt or select voluntary movements. Nevertheless, both motor systems are anatomically interconnected.

5.2. Pathophysiological cerebellar-basal ganglia connectivity

It is generally accepted that there is a close bidirectional connection between the basal ganglia and the cerebellum (Bostan et al., 2010, 2013; Shakkottai et al., 2017). The purpose of our study was to evaluate differences within the communication of the basal ganglia and the cerebellum in dystonic patients compared to controls. Indeed, the putamen facilitated the cerebellum less strong in writer's cramp patients, while the reversed connectivity is only slightly reduced in its facilitating influence on the putamen. In contrast to previous studies that demonstrated only cortico-subcortical abnormal connectivity, it is the aspect of our data that there is also a cerebellar-putaminergic miscommunication in WC, which is bidirectional. These results are in line with a recent study that detected decreased cerebellar connectivity to basal ganglia structures in patients with cervical dystonia (Filip et al., 2017). Most recently, Fuertinger and Simonyan (2017) found evidence for an abnormal functional integration of basal ganglia, cerebellum and thalamus in the laryngeal form of dystonia using a graph theoretical approach (Fuertinger and Simonyan, 2017) and Battistella et al. detected a fragmentation of the functional community between basal ganglia and cerebellum (Battistella et al., 2015). Different from us, the both studies took large-scale functional networks as a basis for their analysis but came to a comparable conclusion concerning the cerebellar- basal ganglia connectivity. However, detailed insight in the pathophysiological bidirectional connectivity is still missing and has to be an objective of future studies.

5.3. Limitations

We investigated the non-affected hand in WC patients in order to get unaffected behavioral data that could be used to build the basis of a valid interpretation of functional data. Therefore, we did not examine the fully blown dystonic network in WC present in the affected hand while writing. However, up to a quarter of patients showed problems in movement execution of the non-affected hand and it has already been suspected by others that network changes within the contralateral hand resemble the pathological motor network present in the affected hand in WC (Wu et al., 2010). In this context, it would be interesting to investigate the bilateral motor network to find possible misbalances between the hemispheres in writer's cramp. A further potential extension of the motor network model is the consideration of the thalamus as an important node within the network. Unfortunately, individual BOLD signal in our data was not strong enough in this area. Namely, an analysis of the BOLD response over all subjects showed an activation of this region, but DCM requires an extraction of the individual time series in a region of interest. Thus, it was not possible to include the thalamus into our network structures. One restriction for the interpretation of the model structure derives from the definition of the model space. As dynamic causal modeling is a hypothesis-driven approach (Stephan et al., 2010). This model space is defined by specifying several plausible models. Given the diverse possibility for connections of the motor network in humans, it is quite likely that we have not found the best model to explain the given data. Therefore, when talking about a “best” or “winner” model in connection with dynamic causal modeling, models outside the actual model space possibly explain the given data better. Therefore, future research should include more or different relevant motor regions, for instance the premotor area or the thalamus. Another limitation results from the definition of the regions of interest. As the choice of ROIs' extent and form are arbitrary, one can find different specifications. The here chosen parameters (4 mm or 6 mm spheres) are inspired by other DCM research done in the field of motor network (Grefkes et al., 2008; Pool et al., 2013; Pool et al., 2014; Tzvi et al., 2014, 2015). Another reason for diverging results in relation to other research outcome is the definition of the ROIs' sphere centers because anatomically different centers potentially lead to other time series that have to be extracted as the basis for each DCM analysis.

6. Conclusion

The network discussed within this study was the first approach examining a network of effective connectivity in WC and resulted in pathophysiological divergences in the cortico-cerebellar and the cortico-basal ganglia loop. The bidirectional connectivity between the motor cortex and the cerebellum was found to be stronger facilitating. In the cortico-basal ganglia circuit the globus pallidus' inhibitory influence on the motor cortex was weakened while the motor cortex inhibited the putamen stronger in WC. Since the behavioral results of the finger-tapping task were comparable between the groups, it is conceivable that patients with WC activate connections within the motor system with more effort to reach the same performance level as healthy subjects.

Further annotations

This research did not receive any specific grant from funding agencies in the public, commercial, or not-for-profit sectors. The authors declare no conflicts of interest.

References

Albanese, A., Bhatia, K., Bressman, S.B., DeLong, M.R., Fahn, S., Fung, V.S.C., ... Teller, J.K., 2013. Phenomenology and classification of dystonia: a consensus update: dystonia: phenomenology and classification. Mov. Disord. 28 (7), 863–873. http://dx.doi.org/10.1002/mds.25475.

Alexander, G.E., Crutcher, M.D., 1990. Functional architecture of basal ganglia circuits: neural substrates of parallel processing. Trends Neurosci. 13 (7), 266–271. http://dx.doi.org/10.1016/0166-2236(90)90107-L.

Battistella, G., Termsarasab, P., Ramdhani, R.A., Fuertinger, S., Simonyan, K., 2015. Isolated focal dystonia as a disorder of large-scale functional networks. Cereb. Cortex, bhv313. http://dx.doi.org/10.1093/cercor/bhv313.

Beck, S., Richardson, S.P., Shamim, E., Dang, N., Schubert, M., Hallett, M., 2008. Short intracortical and surround inhibition are selectively reduced during movement initiation in focal hand dystonia. J. Neurosci. 28 (41), 10363–10369. http://dx.doi.org/10.1523/JNEUROSCI.3564-08.2008.

Blood, A.J., Tuch, D.S., Makris, N., Makhlouf, M.L., Sudarsky, L.R., Sharma, N., 2006. White matter abnormalities in dystonia normalize after botulinum toxin treatment. Neuroreport 17 (12), 1251–1255. http://dx.doi.org/10.1097/01.wnr.0000230500.03330.01.

Bostan, A.C., Dum, R.P., Strick, P.L., 2010. The basal ganglia communicate with the cerebellum. Proc. Natl. Acad. Sci. 107 (18), 8452–8456. http://dx.doi.org/10.1073/pnas.1000496107.

Bostan, A.C., Dum, R.P., Strick, P.L., 2013. Cerebellar networks with the cerebral cortex and basal ganglia. Trends Cogn. Sci. 17 (5), 241–254. http://dx.doi.org/10.1016/j.tics.2013.03.003.

Bradnam, L.V., Graetz, L.J., McDonnell, M.N., Ridding, M.C., 2015. Anodal transcranial direct current stimulation to the cerebellum improves handwriting and cyclic drawing kinematics in focal hand dystonia. Front. Hum. Neurosci. 9 (286). http://dx.doi.org/10.3389/fnhum.2015.00286.

Carbon, M., Ghilardi, M.F., Argyelan, M., Dhawan, V., Bressman, S.B., Eidelberg, D., 2008. Increased cerebellar activation during sequence learning in DYT1 carriers: an equiperformance study. Brain J. Neurol. 131 (Pt 1), 146–154. http://dx.doi.org/10.1093/brain/awm243.

Delmaire, C., Vidailhet, M., Elbaz, A., Bourdain, F., Bleton, J.-P., Sangla, S., ... Lehericy, S., 2007. Structural abnormalities in the cerebellum and sensorimotor circuit in writer's cramp. Neurology 69 (4), 376–380.

Delmaire, C., Vidailhet, M., Wassermann, D., Descoteaux, M., Valabregue, R., Bourdain, F., ... Lehéricy, S., 2009. Diffusion abnormalities in the primary sensorimotor pathways in writer's cramp. Arch. Neurol. 66 (4), 502–508. http://dx.doi.org/10.1001/archneurol.2009.8.

DeLong, M.R., 1990. Primate models of movement disorders of basal ganglia origin. Trends Neurosci. 13 (7), 281–285. http://dx.doi.org/10.1016/0166-2236(90)90110-V.

Doyon, J., Bellec, P., Amsel, R., Penhune, V., Monchi, O., Carrier, J., ... Benali, H., 2009. Contributions of the basal ganglia and functionally related brain structures to motor learning. Behav. Brain Res. 199 (1), 61–75. http://dx.doi.org/10.1016/j.bbr.2008.11.012.

Dresel, C., Li, Y., Wilzeck, V., Castrop, F., Zimmer, C., Haslinger, B., 2014. Multiple changes of functional connectivity between sensorimotor areas in focal hand dystonia. J. Neurol. Neurosurg. Psychiatry 85 (11), 1245–1252. http://dx.doi.org/10.1136/jnnp-2013-307127.

Fahn, S., 1989. Assessment of the primary dystonias. In: The Quantification of Neurologic Deficit. Butterworths, Boston.

Filip, P., Lungu, O.V., Bareš, M., 2013. Dystonia and the cerebellum: a new field of interest in movement disorders? Clin. Neurophysiol. 124 (7), 1269–1276. http://dx.doi.org/10.1016/j.clinph.2013.01.003.

Filip, P., Gallea, C., Lehéricy, S., Bertasi, E., Popa, T., Mareček, R., ... Bareš, M., 2017.

Disruption in cerebellar and basal ganglia networks during a visuospatial task in cervical dystonia. Mov. Disord. 32 (5), 757–768. http://dx.doi.org/10.1002/mds.26930.
Friston, K.J., Harrison, L., Penny, W., 2003. Dynamic causal modelling. NeuroImage 19 (4), 1273–1302. http://dx.doi.org/10.1016/S1053-8119(03)00202-7.
Fuertinger, S., Simonyan, K., 2017. Connectome-wide phenotypical and genotypical associations in focal dystonia. J. Neurosci. 37 (31), 7438–7449. http://dx.doi.org/10.1523/JNEUROSCI.0384-17.2017.
Gallea, C., Herath, P., Voon, V., Lerner, A., Ostuni, J., Saad, Z., ... Hallett, M., 2018. Loss of inhibition in sensorimotor networks in focal hand dystonia. Neuroimage Clin. 17 (Supplement C), 90–97. http://dx.doi.org/10.1016/j.nicl.2017.10.011.
Goldhirsch, I., Sulem, P.-L., Orszag, S.A., 1987. Stability and Lyapunov stability of dynamical systems: a differential approach and a numerical method. Phys. D Nonlinear Phenom. 27 (3), 311–337. http://dx.doi.org/10.1016/0167-2789(87)90034-0.
Granert, O., Peller, M., Jabusch, H.-C., Altenmüller, E., Siebner, H.R., 2011. Sensorimotor skills and focal dystonia are linked to putaminal grey-matter volume in pianists. J. Neurol. Neurosurg. Psychiatry 82 (11), 1225–1231. http://dx.doi.org/10.1136/jnnp.2011.245811.
Grefkes, C., Eickhoff, S.B., Nowak, D.A., Dafotakis, M., Fink, G.R., 2008. Dynamic intra- and interhemispheric interactions during unilateral and bilateral hand movements assessed with fMRI and DCM. NeuroImage 41 (4), 1382–1394. http://dx.doi.org/10.1016/j.neuroimage.2008.03.048.
Hallett, M., 2011. Neurophysiology of dystonia: the role of inhibition. Neurobiol. Dis. 42 (2), 177–184. http://dx.doi.org/10.1016/j.nbd.2010.08.025.
Haslinger, B., Noé, J., Altenmüller, E., Riedl, V., Zimmer, C., Mantel, T., Dresel, C., 2017. Changes in resting-state connectivity in musicians with embouchure dystonia. Mov. Disord. 32 (3), 450–458. http://dx.doi.org/10.1002/mds.26893.
Hikosaka, O., Nakamura, K., Sakai, K., Nakahara, H., 2002. Central mechanisms of motor skill learning. Curr. Opin. Neurobiol. 12 (2), 217–222. http://dx.doi.org/10.1016/S0959-4388(02)00307-0.
Hinkley, L., 2013. Complex-value coherence mapping reveals novel abnormal resting-state functional connectivity networks in task-specific focal hand dystonia. Front. Neurol. 4. http://dx.doi.org/10.3389/fneur.2013.00149.
Hu, X., Wang, L., Liu, H., Zhang, S., 2006. Functional magnetic resonance imaging study of writer's cramp. Chin. Med. J. 119 (15), 1263–1271.
Hubsch, C., Roze, E., Popa, T., Russo, M., Balachandran, A., Pradeep, S., ... Meunier, S., 2013. Defective cerebellar control of cortical plasticity in writer's cramp. Brain 136 (7), 2050–2062. http://dx.doi.org/10.1093/brain/awt147.
Ibáñez, V., Sadato, N., Karp, B., Deiber, M.-P., Hallett, M., 1999. Deficient activation of the motor cortical network in patients with writer's cramp. Neurology 53 (1), 96–105. http://dx.doi.org/10.1212/WNL.53.1.96.
Islam, T., Kupsch, A., Bruhn, H., Scheurig, C., Schmidt, S., Hoffmann, K.-T., 2009. Decreased bilateral cortical representation patterns in writer's cramp: a functional magnetic resonance imaging study at 3.0 T. Neurol. Sci. 30 (3), 219–226. http://dx.doi.org/10.1007/s10072-009-0045-7.
Kasess, C.H., Stephan, K.E., Weissenbacher, A., Pezawas, L., Moser, E., Windischberger, C., 2010. Multi-subject analyses with dynamic causal modeling. NeuroImage 49 (4), 3065–3074. http://dx.doi.org/10.1016/j.neuroimage.2009.11.037.
Kiebel, S.J., Klöppel, S., Weiskopf, N., Friston, K.J., 2007. Dynamic causal modeling: a generative model of slice timing in fMRI. NeuroImage 34 (4), 1487–1496. http://dx.doi.org/10.1016/j.neuroimage.2006.10.026.
Levy, L.M., Hallett, M., 2002. Impaired brain GABA in focal dystonia. Ann. Neurol. 51 (1), 93–101. http://dx.doi.org/10.1002/ana.10073.
Mantel, T., Meindl, T., Li, Y., Jochim, A., Gora-Stahlberg, G., Kräenbring, J., ... Haslinger, B., 2018. Network-specific resting-state connectivity changes in the premotor-parietal axis in writer's cramp. Neuroimage Clin. 17, 137–144. http://dx.doi.org/10.1016/j.nicl.2017.10.001.
Mohammadi, B., Kollewe, K., Samii, A., Beckmann, C.F., Dengler, R., Münte, T.F., 2012. Changes in resting-state brain networks in writer's cramp. Hum. Brain Mapp. 33 (4), 840–848. http://dx.doi.org/10.1002/hbm.21250.
Neychev, V.K., Fan, X., Mitev, V.I., Hess, E.J., Jinnah, H.A., 2008. The basal ganglia and cerebellum interact in the expression of dystonic movement. Brain 131 (9), 2499–2509. http://dx.doi.org/10.1093/brain/awn168.
Odergren, T., Stone-Elander, S., Ingvar, M., 1998. Cerebral and cerebellar activation in correlation to the action-induced dystonia in writer's cramp. Mov. Disord. 13 (3), 497–508. http://dx.doi.org/10.1002/mds.870130321.
Oga, T., Honda, M., Toma, K., Murase, N., Okada, T., Hanakawa, T., ... Shibasaki, H., 2002. Abnormal cortical mechanisms of voluntary muscle relaxation in patients with writer's cramp: an fMRI study. Brain 125 (4), 895–903. http://dx.doi.org/10.1093/brain/awf083.
Oldfield, R.C., 1971. The assessment and analysis of handedness: the Edinburgh inventory. Neuropsychologia 9 (1), 97–113.
Peller, M., Zeuner, K.E., Munchau, A., Quartarone, A., Weiss, M., Knutzen, A., ... Siebner, H.R., 2006. The basal ganglia are hyperactive during the discrimination of tactile stimuli in writer's cramp. Brain 129 (10), 2697–2708. http://dx.doi.org/10.1093/brain/awl181.
Penny, W.D., Stephan, K.E., Daunizeau, J., Rosa, M.J., Friston, K.J., Schofield, T.M., Leff, A.P., 2010. Comparing families of dynamic causal models. PLoS Comput. Biol. 6 (3), e1000709. http://dx.doi.org/10.1371/journal.pcbi.1000709.
Pool, E.-M., Rehme, A.K., Fink, G.R., Eickhoff, S.B., Grefkes, C., 2013. Network dynamics engaged in the modulation of motor behavior in healthy subjects. NeuroImage 82, 68–76. http://dx.doi.org/10.1016/j.neuroimage.2013.05.123.
Pool, E.-M., Rehme, A.K., Fink, G.R., Eickhoff, S.B., Grefkes, C., 2014. Handedness and effective connectivity of the motor system. NeuroImage 99, 451–460. http://dx.doi.org/10.1016/j.neuroimage.2014.05.048.
Preibisch, C., Berg, D., Hofmann, E., Solymosi, L., Naumann, M., 2001. Cerebral activation patterns in patients with writer's cramp: a functional magnetic resonance imaging study. J. Neurol. 248 (1), 10–17. http://dx.doi.org/10.1007/s004150170263.
Rehme, A.K., Eickhoff, S.B., Grefkes, C., 2013. State-dependent differences between functional and effective connectivity of the human cortical motor system. NeuroImage 67, 237–246. http://dx.doi.org/10.1016/j.neuroimage.2012.11.027.
Ridding, M.C., Sheean, G., Rothwell, J.C., Inzelberg, R., Kujirai, T., 1995. Changes in the balance between motor cortical excitation and inhibition in focal, task specific dystonia. J. Neurol. Neurosurg. Psychiatry 59 (5), 493–498. http://dx.doi.org/10.1136/jnnp.59.5.493.
Shakkottai, V.G., Batla, A., Bhatia, K., Dauer, W.T., Dresel, C., Niethammer, M., ... Strick, P.L., 2017. Current opinions and areas of consensus on the role of the cerebellum in dystonia. Cerebellum 16 (2), 577–594. http://dx.doi.org/10.1007/s12311-016-0825-6.
Simonyan, K., Cho, H., Hamzehei Sichani, A., Rubien-Thomas, E., Hallett, M., 2017. The direct basal ganglia pathway is hyperfunctional in focal dystonia. Brain. http://dx.doi.org/10.1093/brain/awx263.
Stephan, K.E., Penny, W.D., Moran, R.J., den Ouden, H.E.M., Daunizeau, J., Friston, K.J., 2010. Ten simple rules for dynamic causal modeling. NeuroImage 49 (4), 3099–3109. http://dx.doi.org/10.1016/j.neuroimage.2009.11.015.
Tzvi, E., Münte, T.F., Krämer, U.M., 2014. Delineating the cortico-striatal-cerebellar network in implicit motor sequence learning. NeuroImage 94, 222–230. http://dx.doi.org/10.1016/j.neuroimage.2014.03.004.
Tzvi, E., Stoldt, A., Witt, K., Krämer, U., 2015. Striatal–cerebellar networks mediate consolidation in a motor sequence learning task: an fMRI study using dynamic causal modelling. NeuroImage 122 (15), 52–64.
Wang, L.E., Fink, G.R., Diekhoff, S., Rehme, A.K., Eickhoff, S.B., Grefkes, C., 2011. Noradrenergic enhancement improves motor network connectivity in stroke patients. Ann. Neurol. 69 (2), 375–388. http://dx.doi.org/10.1002/ana.22237.
Wissel, J., Kabus, C., Wenzel, R., Klepsch, S., Schwarz, U., Nebe, A., ... Poewe, W., 1996. Botulinum toxin in writer's cramp: objective response evaluation in 31 patients. J. Neurol. Neurosurg. Psychiatry 61 (2), 172–175. http://dx.doi.org/10.1136/jnnp.61.2.172.
Wu, C.C., Fairhall, S.L., McNair, N.A., Hamm, J.P., Kirk, I.J., Cunnington, R., ... Lim, V.K., 2010. Impaired sensorimotor integration in focal hand dystonia patients in the absence of symptoms. J. Neurol. Neurosurg. Psychiatry 81 (6), 659–665. http://dx.doi.org/10.1136/jnnp.2009.185637.
Zeuner, K.E., Knutzen, A., Granert, O., Götz, J., Wolff, S., Jansen, O., ... Witt, K., 2015. Increased volume and impaired function: the role of the basal ganglia in writer's cramp. Brain Behav. 5 (2), e00301. http://dx.doi.org/10.1002/brb3.301.